

AperTO - Archivio Istituzionale Open Access dell'Università di Torino

## Lichen Impact on Sandstone Hardness is Species-Specific

**This is a pre print version of the following article:**

*Original Citation:*

*Availability:*

This version is available <http://hdl.handle.net/2318/1834498> since 2023-03-17T16:03:10Z

*Published version:*

DOI:10.1002/esp.5307

*Terms of use:*

Open Access

Anyone can freely access the full text of works made available as "Open Access". Works made available under a Creative Commons license can be used according to the terms and conditions of said license. Use of all other works requires consent of the right holder (author or publisher) if not exempted from copyright protection by the applicable law.

(Article begins on next page)

# 1 **Lichen impact on sandstone hardness is species-specific**

2  
3 Tonon C.<sup>1</sup>, Bernasconi D.<sup>2</sup>, Martire L.<sup>2</sup>, Pastero L.<sup>2</sup>, Viles H.<sup>3</sup>, Favero-Longo  
4 S.E.<sup>1</sup>

5  
6 <sup>1</sup>Department of Life Sciences and Systems Biology, Università degli Studi di  
7 Torino, viale Mattioli 25, 10125 Torino, Italy.

8 <sup>2</sup>Department of Earth Sciences, Università degli Studi di Torino, via Valperga  
9 Caluso 35, 10125 Torino, Italy.

10 <sup>3</sup>School of Geography and the Environment, University of Oxford, South Parks  
11 Road, Oxford, OX1 3QY, UK.

12  
13 email addresses:

14 chiara.tonon@unito.it

15 davide.bernasconi@unito.it

16 luca.martire@unito.it

17 linda.pastero@unito.it

18 heather.viles@ouce.ox.ac.uk

19 sergio.favero@unito.it

20  
21 **Available at:** <https://doi.org/10.1002/esp.5307>

22  
23 **The authors acknowledge for publication on Earth Surface Processes**  
24 **and Landforms (Wiley)**

## 25 26 **Abstract**

27  
28 The balance between lichen biodeterioration and bioprotection processes on  
29 stone surfaces depends on many variables and is crucial to understanding the  
30 role of lichens in biogeomorphology and their threat to stone heritage  
31 conservation. However, stones colonized by lichens have still been mostly  
32 examined in terms of affected volumes and physico-chemical modes of  
33 interactions, overlooking the overall effects on properties related to surface  
34 durability. In this study, the impact of lichen colonization patterns on  
35 Cortemilia sandstone was examined beneath thalli of three lichen species. Rock  
36 hardness, a proxy for rock durability, was measured at different depths from  
37 the surface using an Equotip hardness tester and compared to that of freshly  
38 cut surfaces and exposed surfaces uncolonized by lichens. Mineralogical  
39 analyses were performed by X-ray powder diffraction on rock beneath lichen  
40 colonization, in comparison with unweathered rock. Equotip analyses quantified  
41 a differential, species-specific decrease in stone hardness. This variability was  
42 related to differences in hyphal penetration patterns and, possibly, calcite (re-  
43 )precipitation. In particular, in the case of the species most impacting rock  
44 hardness, X-ray diffraction patterns of calcite showed a remarkable stability of  
45 crystallographic plane (01-12), known to be enhanced in the presence of  
46 organic chelants. These results confirm that decisions on lichen removal from  
47 stone surfaces should consider species-specific behaviour. Moreover, the  
48 innovative approach of measuring stone hardness variation in association with  
49 the analysis of biomineralization processes contributes to unveil the extension

50 of the sphere of lichen interaction within the stone substrate beyond the limit  
51 of the hyphal penetration.

52

53

54 **Keywords:** Biodeterioration, Sandstone, Lichens, Biomineralization, Stone  
55 hardness

## 56 **1. INTRODUCTION**

57

58 Lichens are self-sustaining ecosystems formed by the interaction of an  
59 exhabitant fungus (mycobiont) and an extracellular arrangement of one or  
60 more photosynthetic partners (photobiont(s)) and an indeterminate number of  
61 other microscopic organisms (Hawksworth and Grube, 2020). Saxicolous  
62 lichens represent a remarkable component of lithobiontic communities in many  
63 different environments, ranging from hot and cold deserts to tropical and  
64 temperate areas (Feurerer and Hawksworth, 2007; Wierzchoś *et al.*, 2012). The  
65 thallus of epilithic lichens develops above the surface of stones, which is  
66 penetrated by mycobiont hyphal structures only, while endolithic lichens live  
67 embedded in the mineral substrate, including the photobiont partner, with only  
68 the fruiting structures protruding (Smith *et al.*, 2009). Their colonization of  
69 rock surfaces contributes to weathering processes, supporting pedogenesis and  
70 geomorphic transformation (Jones, 1988; Asplund and Wardle, 2016), but it is  
71 also of relevance for conservation of outdoor stone cultural heritage (Seaward,  
72 2015). Such proven influence on shaping environment, along with their  
73 ubiquity, resulted in the last few decades in a wide interest in characterizing  
74 and modelling processes of interaction between lichens and lithic substrates  
75 (McIlroy de la Rosa *et al.*, 2013).

76 Lichen colonization is generally associated with biodeterioration processes,  
77 which are carefully considered in the case of cultural heritage because of their  
78 negative implications for conservation (Favero-Longo and Viles, 2020).  
79 Adhesion and penetration of lichen structures, together with the release of  
80 acidic and chelating metabolites, have physical and chemical impacts, exerting  
81 mechanical stress and causing dissolution and/or neoformation of minerals  
82 (Salvadori and Casanova-Municchia, 2016). However, at least in some cases,  
83 lichen bioprotection has been also documented, due to their umbrella-like  
84 action against other weathering forces (Carter and Viles, 2004; McIlroy de la  
85 Rosa *et al.*, 2014) or the sealing of rock discontinuities due to  
86 biomineralization (Lee and Parsons, 1999).

87 In this regard, patterns of interactions depend on colonized lithology and lichen  
88 species involved, with their different growth form, penetration, and  
89 metabolome relating to different physical and chemical deteriogenic activities  
90 (Gazzano *et al.*, 2009). Moreover, for the same species and lithologies, the  
91 balance between biodeterioration and bioprotection may change depending on  
92 (micro-)environmental conditions (Carter and Viles, 2004). However, possibly  
93 due to this wide range of variables involved and, in the case of cultural  
94 heritage, the limitations in sampling, stones colonized by lichens have still  
95 been mostly examined in terms of affected volumes and physico-chemical  
96 modes of interactions, overlooking the overall effects on properties related to  
97 durability. Such information is needed to understand the contribution of  
98 saxicolous lichens to biogeomorphology (Viles *et al.*, 2012; Viles, 2020) and  
99 their threats to heritage conservation, addressing choices of removing or  
100 preserving their colonization (Casanova-Municchia *et al.*, 2018).

101 In the case of limestones, lichen colonization has been associated with  
102 counterposed patterns of surface hardening and porosity increase, with their  
103 balance depending on the limestone and the species involved (Morando *et al.*,  
104 2017). Lichen interactions with sandstones -a lithology easily targeted by

105 microbial colonization in nature and widely used in cultural heritage- have been  
106 documented with regard to mycobiont penetration, metabolite release at the  
107 interface and changes in mineral composition (Ariño *et al.*, 1995; Bjelland *et*  
108 *al.*, 2002; Edwards *et al.*, 2002), but investigations have mostly neglected the  
109 consequent influence on rock physico-mechanical properties and potential  
110 divergence from abiotic and other biotic weathering (Jain *et al.*, 2009; Wang *et*  
111 *al.*, 2020).

112 The ability to measure rock hardness, which is considered to be a proxy for  
113 weathering state and durability, developed greatly in the last decade (Wilhelm  
114 *et al.*, 2016b; Kamh and Koltur, 2020). In particular, Equotip devices are  
115 widely recognized as valuable, portable instruments to measure hardness  
116 without the need for destructive sampling. Their application has been  
117 thoroughly studied and calibrated for surface deterioration on a range of  
118 materials including limestone and sandstone (Viles *et al.*, 2011; Wilhelm *et al.*,  
119 2016a; Kovler *et al.*, 2018; Desarnaud *et al.*, 2019; Wang *et al.*, 2020).  
120 Uncertainty about possible limits to the reliability of measures taken in the  
121 proximity of edges, however, has discouraged the application of Equotip to  
122 evaluate hardness on rock cross-sections, although some studies have ruled  
123 out an edge effect, particularly in the case of sandstone (Viles *et al.*, 2011;  
124 Desarnaud *et al.*, 2019). Such a cross-sectional approach may be particularly  
125 fruitful in evaluating the effect on hardness of lithobiontic communities  
126 including lichens, for which measurements on the colonized surfaces, “from the  
127 top”, pose the challenge of removing the biomass without disturbing the  
128 underlying substrate and make it impossible to assay the bioweathering effects  
129 at different depths.

130 This research aimed to examine the impact of lichens on the physico-  
131 mechanical and mineralogical properties of sandstones related to durability. In  
132 particular, we tested the hypotheses that (a) the hardness of sandstones can  
133 be reliably quantified in proximity to block edges, (b) the hardness of  
134 sandstones beneath lichen thalli is lower than that detected without lichen  
135 colonization, and that (c) sandstone hardness at different depths beneath  
136 lichens can vary depending on their growth forms, possibly related to  
137 structural and mineralogical features of the lichen-rock interface. The  
138 investigation was carried out on blocks of Cortemilia sandstone, a lithology of  
139 interest for cultural heritage in NW Italy, colonized by epilithic, endolithic, and  
140 epi- endolithic lichens. Equotip analyses were performed at different depths on  
141 cross-sectioned blocks to evaluate variations in rock hardness. These data  
142 were associated with microscopic characterization of lichen penetration  
143 patterns and lichen-rock interface mineralogical profiles evaluated by X-ray  
144 powder diffraction, to explore possible biogenic interactions responsible for  
145 stone modification.

146

## 147 **2. METHODOLOGY AND METHODS**

148

### 149 **2.1 Stone and lichens**

150 Cortemilia sandstone is quarried in southern Piedmont, Italy, and is employed  
151 extensively in local historical and modern buildings. It is a poorly sorted  
152 sandstone with very fine to medium sized grains, composed of quartz,  
153 feldspar, mica flakes, lithic grains of metamorphic rocks, and carbonate grains

154 locally consisting of bioclasts (Gelati *et al.*, 2010). It originated in middle-late  
155 Burdigalian (early Miocene) (Ghibaudo *et al.*, 2019) from mechanical and  
156 chemical compaction, and displays a limited amount of carbonate cement.  
157 Rock samples were collected from natural outcrops located at the top of a  
158 sunny and xeric hill with sparse trees (upstream the road SP47, Cortemilia,  
159 NW-Italy; WSG84: N 44°33'31.8" - E 8°14'45.3"), choosing or detaching  
160 blocks (n=15) of minimal volume of 1 dm<sup>3</sup>. Selected blocks were colonized by  
161 three crustose lichen species displaying continuous thalli, namely the epilithic  
162 *Verrucaria nigrescens* Pers., the intermediate epi- endolithic *Verrucaria muralis*  
163 Ach. and the endolithic *Protoblastenia incrustans* (DC.) J. Steiner. Surfaces  
164 colonized by scarcely penetrating microbial biofilms, mostly consisting of  
165 cyanobacteria, green algae, and subordinate black fungi, were considered as  
166 weathered controls not exposed to lichen colonization (Morando *et al.*, 2017).  
167 Lichen identification and nomenclature follow Nimis (2016).

168

## 169 **2.2 Equotip hardness testing**

170 Sandstone surface hardness was measured using a Proceq Equotip Piccolo 2  
171 (Proceq, Switzerland) equipped with DL probe, which is very similar to D probe  
172 in terms of impact body diameter (D: 3 mm; DL: 2.78 mm) and energy (D:  
173 11.5 Nmm; DL: 11.1 Nmm), but shows a better correlation with open porosity.  
174 Moreover, due to its geometry, DL is less prone to contamination by dust and  
175 debris which is an issue of relevance when dealing with weathered substrates  
176 (Wilhelm *et al.*, 2016a).

177 Hardness was measured on cross-sectioned surfaces cut with a diamond saw  
178 perpendicularly to lichen thalli, independently of any sandstone stratification,  
179 to expose the lichen-rock interface and the underlying block core. Three out of  
180 the 15 blocks (namely F, J, Z) were further cut to obtain unweathered, right-  
181 angled surfaces, to evaluate the consistency of hardness measures collected  
182 close to block edges (Fig. 1A). Cross-sectioned blocks maintained a  
183 volume >90 cm<sup>3</sup> and a thickness >5 cm, in accord with technical studies and  
184 calibrations reported for Equotip probe D and specifically carried out on  
185 sandstone materials (Corkum *et al.*, 2018; Desarnaud *et al.*, 2019). To avoid  
186 interference due to the presence of moisture contained in the rock (Desarnaud  
187 *et al.*, 2019), the blocks were left to dry for 3 weeks at room temperature to  
188 allow them to reach equilibrium. For the Equotip hardness tests, the blocks  
189 were tightly held in a bench vice, with the section face-up, to ensure surface  
190 stability and reduce as much as possible vibrations during the test.

191 Equotip measurements were carried out (a) at 0.2-0.3 cm from the  
192 unweathered, right-angle surface realized in the block cores (n=3  
193 measurements on independent cross-sections); (b) at 0.2-0.3 cm beneath  
194 each thallus (*V. nigrescens*, n=12; *V. muralis*, n=7; *P. incrustans*, n=8) and  
195 biofilm control (n=12), to evaluate rock hardness as close as possible to the  
196 surface; (c) at 1 cm beneath the same thalli and biofilms, to evaluate  
197 biomodifications affecting stone hardness at greater depth; (d) at the core of  
198 each block, established as the point of the cross section as far as possible, and  
199 always at a minimum distance of 3 cm, from the original block weathered  
200 surfaces. Each measurement consisted of a series of 11 readings, which was  
201 the maximum number of readings obtainable beneath the thalli due to their  
202 limited dimensions and thus consistently adopted for all measurements. The

203 readings were taken in a row, parallel to unweathered edges, lichen thalli and  
204 biofilms (a; b; c) or sparsely in small areas of  $\sim 2,5 \text{ cm}^2$  (d) (Fig. 1B-C).  
205 For each series of readings from the surface layers (a; b; c measurements), a  
206 relative surface hardness value (RSH, *sensu* Aye *et al.*, 2010, Kamh and  
207 Koltuk, 2020) was obtained, that is the ratio between the median value and  
208 the median value of the series of readings from the core of the same block (d  
209 measurement). The value, reported as a percentage (RSH%), represents the  
210 variation of stone hardness due to edge effects (a) and bioweathering (b; c)  
211 compared with unweathered stone hardness (d):

$$\text{RSH}_{\%} = (\text{median}_{\text{surface (a; b; c)}} / \text{median}_{\text{core (d)}}) \times 100 - 100.$$

212  
213  
214 This adjustment avoided the possibility of incorrect interpretations which might  
215 be caused by variability in hardness between different blocks.  
216

217  
218 In order to validate the method of impacting close to an edge (0.2-0.3 cm)  
219 with Equotip Piccolo 2 (probe DL) in the case of Cortemilia sandstone, variation  
220 between hardness measurements close to unweathered edges and their  
221 respective block cores was analysed by Kruskal-Wallis non-parametric test  
222 (Wilhelm *et al.* 2016b), using PAST 4.05 (Hammer *et al.*, 2001). Relative  
223 standard deviation ( $\text{RSD}_{\%} = \text{SD}/\text{Average} \times 100$ , equivalent to "coefficient of  
224 variation") for each series of measurements, excluding the two extreme values  
225 to avoid potential outliers, was also considered.

226 Significant differences in  $\text{RSH}_{\%}$  between the three lichen species and the  
227 control biofilms were tested using non-parametric statistics Kruskal-Wallis and  
228 Mann-Whitney U Test, using PAST 4.05. Data are visualized as box-plots  
229 obtained using Origin(Pro), Version 2021 (OriginLab Corporation,  
230 Northampton, MA, USA).

231

### 232 **2.3 Reflected light microscopy**

233 *V. nigrescens* and *V. muralis* were selected for microscopy observations and  
234 the subsequently described X-ray powder diffraction analysis (*Paragraph 2.4*)  
235 as representative of different lichen impacts on stone hardness. Small  
236 fragments of the sandstone blocks from the lichen-rock interface were  
237 examined to characterise their hyphal penetration within the substrate. The  
238 fragments were cross-sectioned with a diamond saw, embedded in a polyester  
239 resin (R44 Politex-P fast, ICR S.p.A, Italy) and polished with silicon carbide  
240 paper (up to P1200 grit). Hyphal penetration within the substrate was stained  
241 with periodic acid - Schiff's reagent method (PAS; Whitlach and Johnson,  
242 1974) and examined under reflected light (RLM) with an Olympus SZH10  
243 microscope. For each section, the depth of hyphal penetration was quantified,  
244 and the thickness and density of hyphal structures were also observed. Depth  
245 data are reported as box-plots obtained using Origin(Pro), Version 2021.

246

### 247 **2.4 X-ray powder diffraction**

248 X-ray powder diffraction (XRPD) analyses investigated differences in  
249 mineralogical composition beneath *V. muralis* and *V. nigrescens*, compared  
250 with corresponding unweathered core samples. The contents of calcite and  
251 quartz, which are respectively prone and resistant minerals to (bio-)weathering

252 induced-dissolution (Bjelland and Thorseth, 2002), were evaluated for potential  
253 relationships with sandstone hardness. Moreover, calcite was structurally  
254 examined, focusing on the contribution of different crystallographic planes  
255 which may be informative of different crystallization and stabilization  
256 conditions (Klug and Alexander, 1974; Leoni, 2019).

257 Analyses were carried out on four series of samples obtained from the sections  
258 of three of the blocks used for Equotip hardness tests, selecting blocks  
259 colonized by both *V. nigrescens* and *V. muralis* and sampling in the areas of  
260 hardness measurements.

261 For each series, three powder samples were collected from the rock  
262 immediately beneath *V. nigrescens* and *V. muralis* thalli (0.1-0.5 cm from the  
263 surface) and from the block core (at least 3 cm from the surface), respectively.  
264 Sampling was performed using a drill/grinder (Micromot 50/E, Proxxon,  
265 Niersdorf, Germany) equipped with diamond-coated grinding bits, and the  
266 powder was manually ground in an agate mortar. The XRPD patterns were  
267 acquired with a Miniflex 600 diffractometer (Rigaku) operating at 40 kV and 15  
268 mA, using Cu-K<sub>α</sub> radiation (λ=1.5406 Å), in the 2θ range of 3-70°, scan speed  
269 2°/min with step 0.02. Qualitative and semi-quantitative analyses were  
270 performed with SmartLab Studio II v4.3 (Rigaku), using database PDF-  
271 4/Minerals 2020, to recognize main phases and peak heights referred to their  
272 different crystallographic planes.

273 For each XRPD pattern, the peak height (I) and the full-width at half maximum  
274 (FWHM) were calculated for the main peak (10-11) of quartz and the main  
275 (10-14) and six less intense, namely (01-12), (11-20), (11-23), (20-22), (01-  
276 18), (11-26), peaks of calcite. The I/FWHM, which can be used as an indicator  
277 of crystallinity and related to the crystallite size by the Scherrer equation  
278 (Brindley and Brown, 1980), was calculated for each listed peak. The ratio  
279 between the I/FWHM of calcite and quartz was also calculated as follows:

280

$$281 R_{Cc/Qz} = (I_{Cc(10-14)}/FWHM_{Cc(10-14)})/(I_{Qz(10-11)}/FWHM_{Qz(10-11)}).$$

282

283 The relationship between FWHM and material hardness is a standard approach  
284 in material science (Rai *et al.*, 1999; Vashista and Paul, 2012; Fu *et al.*, 2018)  
285 and was assessed using the  $R_{Cc/Qz}$  ratio for *V. nigrescens*, *V. muralis* and block  
286 core samples by a Pearson correlation analysis (PAST 4.05). For each sample  
287 series, the I/FWHM percentage variation of each calcite peak obtained for *V.*  
288 *nigrescens* and *V. muralis* with respect to the core was calculated and  
289 visualized using a Principal Coordinate Analysis plot (PCoA; symmetric scaling,  
290 centring samples by samples, centring species by species, performed using  
291 CANOCO 4.5, Ter Braak and Šmilauer, 2002).

292

### 293 **3. RESULTS**

294

#### 295 **3.1 Consistency of close-to-edge Equotip impacts on Cortemilia** 296 **sandstone**

297 Three independent series of measurements from block cores and unweathered  
298 right-angled surfaces were collected to validate the method of impacting with  
299 Equotip device close to the edge (0.2-0.3 cm) in the case of Cortemilia  
300 sandstone sections.

301 Each block, as expected for sedimentary rocks, was characterised by a  
302 different median hardness value (e.g. variation up to 10.6% between  
303 medians). Within each block however, RSD<sub>%</sub> of both core and edge series of  
304 readings was low (in the range 1.2-3.5%). Median rock hardness measured  
305 close to the edges was lower than that measured in the core, but the  
306 differences were non-significant and lower than 1.2% (Table 1).

307

### 308 **3.2 Rock hardness variation beneath lichens**

309 Hardness variation measured at two depths beneath lichens and the biofilm  
310 control (RSH<sub>%</sub>) indicated a softening of between -1.8% and -17.6% with  
311 respect to the core (Fig. 2). RSH<sub>%</sub> differed significantly beneath the different  
312 lichen species. In particular, at 0.2-0.3 cm, *V. nigrescens* and *P. incrustans*  
313 showed similarly high negative RSH<sub>%</sub> (approx. -17.6%), while *V. muralis*  
314 displayed a significantly lower value (-2.4%). Biofilm control showed  
315 intermediate RSH<sub>%</sub> and a wider range of variation, but the median was closer  
316 to *V. muralis*.

317 At higher depth (1 cm), RSH<sub>%</sub> was generally lower, and was always lower than  
318 closer to the surface (0.2-0.3 cm) for the same species, with the exception of  
319 *V. muralis* (-4.2%). In particular, RSH<sub>%</sub> was particularly low for biofilm control  
320 (-1.8%), while higher for all lichen species, with more evident hardness  
321 variation for *V. nigrescens* (-10.7%) and *P. incrustans* (-8.7%).

322

### 323 **3.3 Hyphal penetration and mineralogical characterization at the** 324 **lichen-rock interface**

325 PAS stained cross sections observed under reflected light microscopy showed  
326 hyphal penetration within Cortemilia sandstone beneath the structurally  
327 different *V. nigrescens* and *V. muralis* thalli, but with different patterns and  
328 depths (Fig. 3).

329 *V. nigrescens* showed a continuous crustose thallus with typical epilithic growth  
330 (Fig. 3B), i.e. with thallus completely above stone surface including photobiont  
331 layer and reproductive structures (perithecia). The mycobiont extensively  
332 penetrated within the stone down to 1.0-1.5 mm, with hyphal network  
333 exploiting intergranular porosity and locally organized as thick bundles (up to  
334 50 µm). Sporadic, thin hyphae were occasionally observed at greater depths.  
335 The continuous, crustose thallus of the epi- endolithic *V. muralis* was poorly  
336 developed above the surface, showing photobiont clusters aligned at the rock  
337 surface and perithecia partially immersed in the substrate (Fig. 3C). Its  
338 mycobiont penetrated extensively down to 1.2-1.3 mm and occasionally to  
339 greater depths, as observed for *V. nigrescens*, but with less dense and thinner  
340 hyphae, only rarely organized as bundles. In a couple of cases, the early 200-  
341 300 µm beneath the algal layer appeared quite free of hyphae and seemingly  
342 more compact, while mycobiont diffusely penetrated in the millimeter below.

343 XRPD analyses displayed similar R<sub>Cc/Qz</sub> values for all the samples, ranging  
344 between 0.33 and 0.72, with the exception of two core samples with R<sub>Cc/Qz</sub>  
345 higher than 1.75. No significant differences between *V. nigrescens* and *V.*  
346 *muralis* were observed. The relationship among R<sub>Cc/Qz</sub> and stone hardness is  
347 shown in Fig. 4A. A slight, non significant, negative correlation was observed  
348 for both the species (R=-0.2; P=>0.05).

349 The PCoA (Fig. 4B) extracted three components which explained 100% of total

350 variance and ordinated samples collected beneath lichens on the basis of the  
351 percentage variation of I/FWHM ratio of each calcite peak with respect to the  
352 relative core sample. The first axis (69.9% of total variance) displayed its  
353 highest positive correlation with (01-12) crystallographic plane and with  
354 samples collected beneath *V. nigrescens* showing lowest hardness values.  
355 Oppositely, samples with highest negative correlation with (01-12) showed the  
356 highest hardness.

357

#### 358 **4. DISCUSSION**

359 Analysis of lichen-rock interaction patterns may not fully clarify the balance  
360 between lichen bioweathering and bioprotection, particularly at the species  
361 specific level, which determines their biogeomorphological role (McIlroy de la  
362 Rosa *et al.*, 2013) and should contribute to decisions about whether to remove  
363 or preserve lichens on heritage surfaces (Casanova-Municchia *et al.*, 2018).  
364 Measurements of rock hardness, as a proxy of surface durability vs. erodibility  
365 (Wilhelm *et al.*, 2016b), have recently been applied to studies of sandstone  
366 weathering, encompassing lichen colonization as a general phenomenon rather  
367 than focusing on the complexity of lichen-rock interaction and species specific  
368 patterns (Kamh and Koltuk, 2020). In our investigation, we proved the efficacy  
369 of a protocol of hardness measurements at the lichen-rock interface,  
370 particularly verifying the hypothesis of (a) a non-significant influence of  
371 measuring in proximity to block edges for the examined sandstone. With such  
372 an approach, we verified the hypotheses of (b) a significant hardness variation  
373 at different depths beneath lichen thalli with respect to a biofilm control, and of  
374 (c) the differential hardness variation as a species-specific phenomenon, which  
375 cannot be directly related to epilithic or endolithic growth forms. In the  
376 following sub-sections, we discuss the adopted method to measure hardness  
377 variation with respect to most recent protocols calibrated for analyses of  
378 sandstone weathering, also taking into consideration limitations due to  
379 sampled material, variability in sandstones, and lichen thalli dimensions  
380 (*Paragraph 4.1*). Thereafter, we disentangle the patterns and species-  
381 specificity of lichen impact on a calcareous sandstone hardness (*Paragraph*  
382 *4.2*), and we address insights on the relationship between species-specific  
383 physico-chemical modes of lichen interaction, i.e. hyphal penetration and  
384 biomineralization, and their effect on durability (*Paragraph 4.3*).

385

##### 386 **4.1 Suitability of measuring hardness along sandstone cross-sections**

387 The method of measuring hardness on cross-sections of lichen colonized  
388 sandstone, including measurements close to block edges, is here proposed  
389 following previous protocols applied on fresh cut, unweathered sandstones  
390 (Desarnaud *et al.*, 2019) and on the surface of lichen colonized rocks (e.g.  
391 limestone, Morando *et al.*, 2017; sandstone, Kamh and Koltuk, 2020). Such  
392 previous protocols involving Equotip readings directly on colonized surfaces,  
393 however, reflected a cushion-like effect of the lichen biomass when thalli were  
394 not preliminarily removed. Alternatively, they required careful removal of a  
395 thallus (Morando *et al.*, 2017), which for some lithologies, as sandstone,  
396 cannot be performed without affecting the substrate. Such limitations are  
397 overcome with our implemented method of collecting measurements directly  
398 from beneath lichen thalli or other lithobionts. This confers advantages related

399 to the possibility of obtaining innovative information of biological influence on  
400 stone properties at different depths, including the first millimetres from stone-  
401 atmosphere interface. In particular, we showed that 0.2-0.3 cm from edges  
402 obtained by sectioning blocks is a suitable distance for the Equotip probe  
403 geometry, which still ensures a reliable measurement not significantly different  
404 from (almost equivalent to) that collected at the block core. Similarly, Viles  
405 and colleagues (2011) did not observe any edge-effect for Equotip applications  
406 on sandstones, although these have been detected for other lithologies, such  
407 as granite, concrete and limestone (Coombes *et al.*, 2013), suggesting the  
408 necessity of validating the cross-section approach on each lithology of interest.  
409 Sampling of different sandstone blocks in a natural environment implied issues  
410 related to a high variability due to different sedimentary layers, orientation,  
411 aspect, time of surface exposure, and other uncontrolled factors (e.g. Yun *et al.*,  
412 2013). Moreover, Equotip measurements on different blocks were not  
413 always taken perpendicularly to sedimentary layers (Desarnaud *et al.*, 2019),  
414 but depending on the surface colonized by lichens and, consequently, its cross-  
415 section orientation. To balance out this variability, measurements were  
416 normalized to the core of each block, used as internal comparison. It was  
417 indeed not possible to obtain measurements of unweathered rock at the same  
418 0.2-0.3 cm distance from the surface due to general and variable surface  
419 weathering independent of lichens.

420

#### 421 **4.2 Stone hardness variation beneath lichens**

422 Hardness variation -with respect to the core- beneath lichens and the biofilm  
423 control always showed higher negative values (from -2 to -17%) than that  
424 detected beneath unweathered, right-angle edges (< -1.2%). Accordingly, the  
425 closeness to the atmosphere-rock interface and the consequent exposure to  
426 biotic and abiotic weathering agents (Gorbushina and Broughton, 2009), rather  
427 than the geometry of the surfaces related to cross sectioning, accounts for  
428 hardness variation. More remarkably, the highest hardness variation is  
429 detected beneath two of the assayed lichen species, confirming and quantifying  
430 a prominent role of lichens in rock deterioration with respect to other  
431 lithobionts (St. Clair and Seaward, 2004; Salvadori and Casanova-Municchia,  
432 2016; Morando *et al.*, 2017).

433 The crustose thalli of the investigated lichen species share the absence of  
434 secreted compounds, as oxalic acid and acidic and/or chelating secondary  
435 metabolites known for their deteriorogenic activity, while they are characterized  
436 by a different structural organization (Nimis, 2016). Noteworthy, hardness  
437 variation was similar beneath the epilithic *V. nigrescens* and the endolithic *P.*  
438 *incrustans*, rejecting the hypothesized higher biodeterioration by endolithic  
439 lichens due to their life completely embedded in the substrate (Caneva *et al.*,  
440 2008), but also their direct correlation with bioprotective effects (Gadd and  
441 Dyer, 2017). In detail, the hardness variation beneath these lichens is similarly  
442 high at 0.2-0.3 cm (-17.6%) and still remarkable (approx. -10%) at 1 cm,  
443 suggesting an equivalent impact for the two species on the investigated  
444 sandstone.

445 The detectable hardness variation at 1 cm beneath lichens is particularly  
446 remarkable with respect to the null variation driven by biofilm control with  
447 respect to the unweathered core, highlighting the deep impact of certain lichen

448 species. Instead, at 0.2-0.3 cm, some negative hardness variation was also  
449 detected beneath the biofilm control (-6%), with higher variability possibly  
450 related to the heterogeneous biofilm composition on the different blocks.  
451 Nevertheless, a general influence of surface processes, including abiotic  
452 weathering, cannot be ruled out, as they can also significantly impact  
453 sandstone hardness (Kamh and Koltur, 2020), but their effect is more  
454 superficial than that induced by lichens.

455 In a very different manner, a significantly lower variation in hardness was  
456 detected beneath the epi- endolithic *V. muralis*. This was remarkably  
457 significant at 0.2-0.3 cm depth, while the variation slightly increased and  
458 reached values more similar to those of the other species at 1 cm depth. This  
459 phenomenon may suggest not a simple lower impact of *V. muralis* on stone  
460 hardness, but even some form of hardening process, which likely compensate,  
461 at least in part, stone softening caused by hyphal penetration (see below).  
462 Accordingly, hardening processes were shown for some lichen species on  
463 limestone, and in the case of Botticino limestone the epi- endolithic  
464 *Xanthocarpia ochracea* was associated with unmodified hardness with respect  
465 to fresh rock where *V. nigrescens* determined hardness lowering (Morando *et*  
466 *al.*, 2017).

467

#### 468 **4.3 Insights on the basis of species-specific lichen impact**

469 Different patterns of hardness variation were evaluated by comparing aspects  
470 of physico-chemical interactions of the epi- endolithic *V. muralis* with the  
471 Cortemilia sandstone with respect to the genetically related, but epilithic *V.*  
472 *nigrescens*.

473 Hyphal penetration down to millimetric depths was often reported for different  
474 sandstone lithologies (Chen *et al.*, 2000). The highest penetration values here  
475 observed for both species agreed with similar previous reports, but the  
476 massive penetration mostly affected the first millimeter only. In this regard,  
477 textural features, including porosity, have been recognized as first  
478 determinants of the rock susceptibility to colonization and, particularly, to  
479 hyphal penetration (Camara *et al.*, 2008). The absence of significant  
480 interspecific variability in hyphal penetration between *V. nigrescens* and *V.*  
481 *muralis* likely reflects the availability of passageways in the first upper  
482 millimeter, although it is always difficult to ascertain whether hyphae exploit  
483 existing discontinuities and actively contribute to produce new fissures (Ascaso  
484 and Wierzchoś, 1995). Surface layers of sandstones beneath lichens displayed  
485 a porosity due to dissolution of calcite and other poorly stable minerals  
486 (Bjelland and Thorseth, 2002). Accordingly, XRPD analyses showed strongly  
487 higher  $R_{Cc/Qz}$  for two core samples with respect to the related volumes beneath  
488 both the *Verrucaria* species, indicating some calcite dissolution. The absence of  
489 surfaces free of lichen or microbial colonization, however, prevented the  
490 possibility of verifying if such pattern is directly related to biological activity or  
491 is related to abiotic weathering factors, pre-dating lichen colonization  
492 (Turkington and Paradise, 2005). For the other two sample series, the low  
493  $R_{Cc/Qz}$  characterized for core samples, equal to that obtained for volumes  
494 beneath lichens, likely reflects an initial lower content of calcite, whose amount  
495 is known to vary in the Cortemilia sandstone (Gnaccolini and Rossi, 1994). In  
496 all cases, however,  $R_{Cc/Qz}$  neither showed significant correlation with stone

497 hardness nor explained different hardness beneath the two lichen species,  
498 excluding that calcite dissolution alone accounts for the hardness variation with  
499 respect to the core. Moreover, a partial dissolution, rather than the complete  
500 absence of calcite reported by Bjelland and Thorseth (2002), was detected  
501 through the whole set of samples collected in the 5 mm deep layer beneath the  
502 lichen thalli. Although a bioprotective umbrella-effect of lichen thalli on calcite-  
503 rich lithologies was experimentally demonstrated (McIlroy de la Rosa *et al.*,  
504 2014), such heterogeneity explains that many other factors, dealing with the  
505 overall history of stone surfaces, may account for their currently observable  
506 physico-chemical properties and the consequent conservation condition.  
507 It is worth noting that maximum values of massive penetration were observed  
508 for *V. nigrescens*, which also displayed a denser hyphal presence in the  
509 penetrated layer, with hyphal bundles and thicker hyphal network. Such  
510 penetration patterns are consistent with pervasive penetration observed for *V.*  
511 *nigrescens* within limestone (Favero-Longo *et al.*, 2009), which was related to  
512 its high negative impact on limestone hardness (Morando *et al.*, 2017).  
513 Anyway, these slight differences between *V. nigrescens* and *V. muralis* are  
514 unlikely to explain different hardness variations beneath the two species,  
515 mostly because hyphal penetration only rarely affected the stone deeper than  
516 2 mm, while close-to-surface hardness measurements were collected at 0.2-  
517 0.3 cm from the surface. The detected penetration patterns seem thus to  
518 reject the hypothesis of an exclusive role of the mechanical action of hyphae in  
519 determining stone hardness modification.  
520 Higher heating of rock surfaces beneath *V. nigrescens* with respect to white  
521 lichen thalli was also indicated as responsible for the high stress rate induced  
522 on rock stability (Carter and Viles, 2004). However, XRPD analyses added  
523 further insights on the biogeochemical side of lichens-sandstone interaction. As  
524 expected, oxalates were absent (or below the XRPD detection limit) beneath  
525 both the epi- and epi- endolithic *Verrucaria* thalli. Accordingly, oxalic acid -  
526 recognized as a factor responsible for bioweathering by other lichen species on  
527 sandstone (Edwards *et al.*, 2002)- is not a driver of the biodeterioration  
528 induced by Verrucariales, as already ascertained for endolithic species of the  
529 order (Pinna *et al.*, 1998) (Pinna *et al.*, 1998) with the exception of *Verrucaria*  
530 *rubrocincta* (Bungartz *et al.*, 2004). The different peaks of calcite are instead  
531 informative on the stability of different crystallographic planes, which are  
532 known to be differently enhanced in presence of organic substance (Klug and  
533 Alexander, 1974; Leoni, 2019). In particular, calcite form (01-12) is stabilized  
534 by organic chelants (Pastero *et al.*, 2003). Accordingly, the correlation between  
535 the lowest hardness values observed beneath *V. nigrescens* and (01-12) may  
536 be explained by exposure of the assayed stone volumes to organic chelants,  
537 indicating that lichen impact on the stone extended beyond the hyphal  
538 penetrated volume through metabolite release. Although the production of  
539 lichen secondary metabolites is not a trait of Verrucariales, the release of  
540 chelating compounds was already observed for endolithic species (Favero-  
541 Longo *et al.*, 2011) and may be a more widely shared feature, which does not  
542 leave prominent traces as oxalates. In this sense, we cannot exclude the  
543 possibility that *V. muralis* also releases metabolites affecting the rock stability,  
544 but the phenomenon is not reflected in the observed calcite crystallization and,  
545 if it exists, may be more limited in line with the poorly developed biomass,

546 above and within the substrate.

547 Dissolution and re-precipitation of calcite associated with lichen colonization  
548 was already characterized for endolithic species and associated with a  
549 respiration-induced acidification pathway (Weber *et al.*, 2011). Lichen  
550 biomineralization of micrite was recognized as a bioprotection factor,  
551 counterbalancing the deterioration induced by hyphal penetration (Bungartz *et*  
552 *al.*, 2004). The same presence of organic matter may be the cause of  
553 hardening of upper rock layers, as already demonstrated for microbial biofilms  
554 (Slavik *et al.*, 2017), but still poorly explored for lichens (Morando *et al.*,  
555 2017). Our analyses did not allow us to exclude the possibility that the low  
556 impact of *V. muralis* on rock hardness may result from similar re-precipitation  
557 and hardening processes, as suggested by the observation of a layer appearing  
558 more compact just beneath the algal clusters, whose investigation will be the  
559 object of a subsequent contribution.

560

## 561 **5. CONCLUSIONS**

562 This investigation showed that each lichen species may have a different impact  
563 on physico-mechanical properties of sandstones, as measured by surface  
564 hardness, a proxy for durability. Accordingly, a reliable evaluation of  
565 biogeomorphological processes affecting sandstone cannot generalize lichen  
566 contributions as biodeteriorative or bioprotective, or univocally associate a  
567 certain effect with the epilithic and endolithic growth forms, but rather needs  
568 to disentangle and summarize the heterogeneous contributions of different  
569 species. Such species-specific patterns are known -and here confirmed- to  
570 depend on the balance between several mechanisms of physico-mechanical  
571 and chemical impact which positively or negatively impact substrate durability.  
572 However, chemical processes may not always leave prominent evidence of  
573 their occurrence and extension at depth, as in the case of the investigated  
574 species which do not produce oxalate deposits. Our analyses suggested that  
575 microscopy observations may be integrated with mineralogical investigations,  
576 to unveil the extension of the sphere of lichen interaction within the rock  
577 substrate beyond the limit of hyphal penetration, by highlighting deeper traces  
578 of biomineralization processes. Such findings are also of relevance in the field  
579 of cultural heritage conservation, indicating that decisions on the preservation  
580 or removal of lichens, as agents of biodeterioration or bioprotection, cannot be  
581 generalized, but should carefully consider the behaviour of each species, at  
582 least focusing on dominant ones.

583

## 584 **REFERENCES**

585 Ariño, X., Ortega-Calvo, J.J., Gomez-Bolea, A. and Saiz-Jimenez, C. (1995)  
586 Lichen colonization of the Roman pavement at Baelo Claudia (Cadiz, Spain):  
587 Biodeterioration vs. bioprotection. *Sci. Total Environ.*, 167, 353-363. Available  
588 at: doi:10.1016/0048-9697(95)04595-R.  
589 Ascaso, C. and Wierzchoś, J. (1995) Study of the biodeterioration zone  
590 between the lichen thallus and the substrate. *Crypt. Bot.*, 5, 270-281.  
591 Available at: [http://digital.csic.es/bitstream/10261/32346/1/CB5\\_270.pdf](http://digital.csic.es/bitstream/10261/32346/1/CB5_270.pdf).  
592 Asplund, J. and Wardle, D.A. (2016) How lichens impact on terrestrial  
593 community and ecosystem properties. *Biol. Rev.*, 92, 1720-1738. Available at:  
594 doi:10.1111/brv.12305.

595 Aye, T., Oguchi, C.T. and Takaya, Y. (2010) Evaluation of sulfate resistance of  
596 Portland and high alumina cement mortars using hardness test. *Constr. Build.*  
597 *Mater.*, 24, 1020-1026. Available at: 10.1016/j.conbuildmat.2009.11.016.

598 Bjelland, T., Sabo, L. and Thorseth, I.H. (2002) The occurrence of  
599 biomineralization products in four lichen species growing on sandstone in  
600 western Norway. *The Lichenologist*, 34, 429-440. Available at:  
601 doi:10.1006/lich.2002.0413.

602 Bjelland, T. and Thorseth, I.H. (2002) Comparative studies of the lichen-rock  
603 interface of four lichens in Vingen, western Norway. *Chem. Geol.*, 192, 81-98.  
604 Available at: doi:10.1016/S0009-2541(02)00193-6.

605 Brindley, G.W. and Brown, G. (1980) *Crystal structures of clay minerals and*  
606 *their X-ray identification*. Mineralogical Society of Great Britain and Ireland,  
607 Colchester and London.

608 Bungartz, F., Garvie, L.A.J. and Nash III, T.H. (2004) Anatomy of the  
609 endolithic Sonoran Desert lichen *Verrucaria rubrocincta* Breuss: Implications  
610 for biodeterioration and biomineralization. *The Lichenologist*, 36, 55-73.  
611 Available at: doi:10.1017/S0024282904013854.

612 Camara, B., de los Rios, A., Garcia del Cura, M.A., Galvan, V. and Ascaso, C.  
613 (2008) Dolostone bioreceptivity to fungal colonization. *Materiales De*  
614 *Construcción*, 58, 113-124. Available at: doi:10.3989/mc.2008.v58.i289-  
615 290.71.

616 Caneva, G., Nugari, M.P., and Salvadori, O. (2008) *Plant biology for cultural*  
617 *heritage: Biodeterioration and conservation*. Getty Publications, Los Angeles,  
618 California.

619 Carter, N.E.A. and Viles, H. (2004) Lichen hotspots: Raised rock temperatures  
620 beneath *Verrucaria nigrescens* on limestone. *Geomorphology*, 62, 1-16.  
621 Available at: doi:10.1016/j.geomorph.2004.02.001.

622 Casanova-Municchia, A., Bartoli, F., Taniguchi, Y., Giordani, P. and Caneva, G.  
623 (2018) Evaluation of the biodeterioration activity of lichens in the Cave Church  
624 of Uzumlu (Cappadocia, Turkey). *Int. Biodeterior. Biodegrad*, 127, 160-169.  
625 Available at: doi:10.1016/j.ibiod.2017.11.023.

626 Chen, J., Blume, H.P. and Beyer, L. (2000) Weathering of rocks induced by  
627 lichen colonization - A review. *Catena*, 39, 121-146. Available at:  
628 doi:10.1016/S0341-8162(99)00085-5.

629 Coombes, M.A., Feal-Perez, A., Naylor, L.A. and Wilhelm, K. (2013) A  
630 nondestructive tool for detecting changes in the hardness of engineering  
631 materials: Application of the Equotip durometer in the coastal zone. *Eng. Geol.*,  
632 167, 14-19. Available at: doi:10.1016/j.enggeo.2013.10.003.

633 Corkum, A.G., Asiri, Y., El Naggar, H. and Kinakin, D. (2018) The Leeb  
634 hardness test for rock: An updated methodology and UCS correlation. *Rock*  
635 *Mech. Rock Eng.*, 51, 665-675. Available at: doi:10.1007/s00603-017-1372-2.

636 Desarnaud, J., Kiriya, K., Bicer Simsir, B., Wilhelm, K. and Viles, H. (2019)  
637 A laboratory study of Equotip surface hardness measurements on a range of  
638 sandstones: What influences the values and what do they mean? *Earth Surf.*  
639 *Process. Landforms*, 44, 1419-1429. Available at: doi:10.1002/esp.4584.

640 Edwards, H.G., Holder, J.M., Seaward, M.R. and Robinson, D.A. (2002) Raman  
641 spectroscopic study of lichen- assisted weathering of sandstone outcrops in  
642 the High Atlas Mountains, Morocco. *J. Raman Spectrosc.*, 33, 449-454.  
643 Available at: doi:10.1002/jrs.859.

644 Favero-Longo, S.E., Borghi, A., Tretiach, M. and Piervittori, R. (2009) *In vitro*  
645 receptivity of carbonate rocks to endolithic lichen-forming aposymbionts.  
646 *Mycol. Res.*, 113, 1216-1227. Available at: doi:10.1016/j.mycres.2009.08.006.  
647 Favero-Longo, S.E., Gazzano, C., Girlanda, M., Castelli, D., Tretiach, M.,  
648 Baiocchi, C. and Piervittori, R. (2011) Physical and chemical deterioration of  
649 silicate and carbonate rocks by meristematic microcolonial fungi and endolithic  
650 lichens (Chaetothyriomycetidae). *Geomicrobiol. J.*, 28, 732-744. Available at:  
651 doi:10.1080/01490451.2010.517696.  
652 Favero-Longo, S.E. and Viles, H. (2020) A review of the nature, role and  
653 control of lithobionts on stone cultural heritage: Weighing up and managing  
654 biodeterioration and bioprotection. *World J. Microbiol. Biotechnol.*, 36, 1-18.  
655 Available at: doi:10.1007/s11274-020-02878-3.  
656 Feuerer, T. and Hawksworth, D.L. (2007) Biodiversity of lichens, including a  
657 worldwide analysis of checklist data based on Takhtajan's Xoristic regions.  
658 *Biodivers. Conserv.*, 16, 85-98. Available at: doi:10.1007/s10531-006-9142-6.  
659 Fu, P., Chu, R., Xu, Z., Ding, G. and Jiang, C. (2018) Relation of hardness with  
660 FWHM and residual stress of GCr15 steel after shot peening. *Appl. Surf. Sci.*,  
661 431, 165-169. Available at: doi:10.1016/j.apsusc.2017.09.136.  
662 Gadd, G.M. and Dyer, T.D. (2017) Bioprotection of the built environment and  
663 cultural heritage. *Microb. Biotechnol.*, 10, 1152-1156. Available at:  
664 doi:10.1111/1751-7915.12750.  
665 Gazzano, C., Favero-Longo, S.E., Matteucci, E. and Piervittori, R. (2009)  
666 Image analysis for measuring lichen colonization on and within stonework. *The*  
667 *Lichenologist*, 41, 299-313. Available at: doi:10.1017/S0024282909008366.  
668 Gelati, R., Gnaccolini, M., Polino, R., Mosca, P., Piana, F., Fioraso, G., Balestro,  
669 G., Tallone, S., Ramasco, M., Fontan, D., Sorzana, P., Campus, S. and Ossella,  
670 L. (2010) Note illustrative della Carta Geologica d'Italia alla scala 1:50000,  
671 Foglio 211 Dego. *ISPRA Istituto Superiore per la Protezione e la Ricerca*  
672 *Ambientale*. Available at:  
673 [https://www.isprambiente.gov.it/Media/carg/note\\_illustrative/211\\_Dego.pdf](https://www.isprambiente.gov.it/Media/carg/note_illustrative/211_Dego.pdf).  
674 Ghibaud, G., Massari, F., Chiambretti, I., d'Atri, A. and Fornaciari, E. (2019)  
675 Birth and tectono-sedimentary evolution of the Tertiary Piedmont Basin (NW  
676 Italy). *J. Mediterr. Earth Sci.*, 11, Spec. Issue, 5-112. Available at:  
677 doi:10.3304/JMES.2019.008.  
678 Gnaccolini, M. and Rossi, P.M. (1994) Depositional sequences and sandstone  
679 composition in the Tertiary Piedmont basin: Preliminary results. *Atti Tic. Sc.*  
680 *Terra*, 37, 3-15.  
681 Gorbushina, A.A. and Broughton, W.J. (2009) Microbiology of the atmosphere-  
682 rock interface: How biological interactions and physical stresses modulate a  
683 sophisticated microbial ecosystem. *Annu. Rev. Microbiol.*, 63, 431-450.  
684 Available at: doi:10.1146/annurev.micro.091208.073349.  
685 Hammer, O., Harper, D.A.T. and Ryan, P.D. (2001) PAST: Paleontological  
686 statistics software package for education and data analysis. *Paleontol.*  
687 *Electronica*, 4, 1-9. Available at: [http://palaeo-](http://palaeo-electronica.org/2001_1/past/issue1_01.htm)  
688 [electronica.org/2001\\_1/past/issue1\\_01.htm](http://palaeo-electronica.org/2001_1/past/issue1_01.htm).  
689 Hawksworth, D.L. and Grube, M. (2020) Lichens redefined as complex  
690 ecosystems. *New Phytol.*, 227, 1281-1283. Available at:  
691 doi:10.1111/nph.16630.  
692 Jain, A., Bhadauria, S., Kumar, V. and Singh Chauhan, R. (2009)

693 Biodeterioration of sandstone under the influence of different humidity levels in  
694 laboratory conditions. *Build. Environ.*, 44, 1276-1284. Available at:  
695 doi:10.1016/j.buildenv.2008.09.019.

696 Jones, D. (1988) Lichens and pedogenesis. In: Galun M. (Ed.) *CRC Handbook*  
697 *of Lichenology*. CRC Press, Boca Raton, Florida, pp. 109-124.

698 Kamh, G.M.E. and Koltuk, S. (2020) Variation of micro topographic and  
699 geotechnical limits on weathering progress on the constructional Triassic  
700 sandstone, Aachen city, Germany, case study. *Environ. Earth Sci.*, 79, 1-13.  
701 Available at: doi:10.1007/s12665-020-09263-1.

702 Klug, H.P. and Alexander, L.E. (1974) *X-ray diffraction procedures: for*  
703 *polycrystalline and amorphous materials*. Wiley-Interscience, New York.

704 Kovler, K., Wang, F. and Muravin, B. (2018) Testing of concrete by rebound  
705 method: Leeb *versus* Schmidt hammers. *Mater. Struct.*, 51, 1-14. Available at:  
706 doi:10.1617/s11527-018-1265-1.

707 Lee, M.R. and Parsons, I. (1999) Biomechanical and biochemical weathering of  
708 lichen-encrusted granite: Textural controls on organic-mineral interactions and  
709 deposition of silica-rich layers. *Chem. Geol.*, 161, 385-397. Available at:  
710 doi:10.1016/S0009-2541(99)00117-5.

711 Leoni, M. (2019) Domain size and domain-size distributions. In: Gilmore C.J.,  
712 Kaduk, J.A. and Schenk, H. (Eds.) *International Tables for Crystallography*  
713 *Volume H: Powder Diffraction*. pp. 524-537. Available at:  
714 doi:10.1107/97809553602060000966.

715 McIlroy de la Rosa, J.P., Warke, P.A. and Smith, B.J. (2013) Lichen-induced  
716 biomodification of calcareous surfaces: Bioprotection *versus* biodeterioration.  
717 *Prog. Phys. Geogr.*, 37, 325-351. Available at:  
718 doi:10.1177/0309133312467660.

719 McIlroy de la Rosa, J.M., Warke, P.A. and Smith, B.J. (2014) The effects of  
720 lichen cover upon the rate of solutional weathering of limestone.  
721 *Geomorphology*, 220, 81-92. Available at:  
722 doi:10.1016/j.geomorph.2014.05.030.

723 Morando, M., Wilhelm, K., Matteucci, E., Martire, L., Piervittori, R., Viles, H.  
724 and Favero-Longo, S.E. (2017) The influence of structural organization of  
725 epilithic and endolithic lichens on limestone weathering. *Earth Surf. Process.*  
726 *Landforms*, 42, 1666-1679. Available at: doi:10.1002/esp.4118.

727 Nimis P.L. (2016) *ITALIC, The Information System on Italian Lichens*. Version  
728 5.0. University of Trieste, Dept. of Biology. Available at:  
729 <http://dryades.units.it/italic> [Accessed 23 September 2020].

730 Pastero, L., Costa, E., Alessandria, B., Rubbo, M. and Aquilano, D. (2003) The  
731 competition between {10-14} cleavage and {01-12} steep rhombohedra in gel  
732 grown calcite crystals. *J. Cryst. Growth*, 247, 472-482. Available at:  
733 doi:10.1016/S0022-0248(02)01911-5.

734 Pinna, D., Salvadori, O. and Tretiach, M. (1998) An anatomical investigation of  
735 calcicolous endolithic lichens from the Trieste karst (NE Italy). *Plant*  
736 *Biosystems*, 132, 183-195. Available at:  
737 doi:10.1080/11263504.1998.10654203.

738 Rai, S., Choudhary, B.K., Jayakumar, T., Rao, K.B.S. and Raj, B. (1999)  
739 Characterization of low cycle fatigue damage in 9Cr-1Mo ferritic steel using X-  
740 ray diffraction technique. *Int. J. Pres. Ves. Pip.*, 76, 275-281. Available at:  
741 10.1016/S0308-0161(98)00140-9.

742 Salvadori, O. and Casanova-Municchia, A. (2016) The role of fungi and lichens  
743 in the biodeterioration of stone monuments. In: *The Open Conference*  
744 *Proceedings Journal*, 7, 39-54. Available at:  
745 doi:10.2174/2210289201607020039.

746 Seaward, M.R.D. (2015) Lichens as agents of biodeterioration. In: Kumar  
747 Upreti, D., Divakar, P.K., Shukla, V. and Bajpai, R. (Eds.) *Recent advances in*  
748 *lichenology*. Springer, New Delhi, pp. 189-211.

749 Šlavik, M., Bruthans, J., Filippi, M., Schweigstillova, J., Falteisek, L. and  
750 Rihošek, J. (2017) Biologically-initiated rock crust on sandstone: Mechanical  
751 and hydraulic properties and resistance to erosion. *Geomorphology*, 278, 298-  
752 313. Available at: doi:10.1016/j.geomorph.2016.09.040.

753 Smith, C.W., Aptroot, A., Coppins, B.J., Fletcher, A., Gilbert, O.L., James, P.W.  
754 and Wolseley P.A. (2009) *Lichens of Great Britain and Ireland*. British Lichen  
755 Society, London. St. Clair, L.L. and Seaward, M.R.D. (2004) *Biodeterioration of*  
756 *stone surface: Lichen and biofilms as weathering agents of rocks and cultural*  
757 *heritage*. Kluwer Academic Publishers, Dordrecht.

758 Ter Braak, C.J. and Smilauer, P. (2002) *CANOCO reference manual and*  
759 *CanoDraw for Windows user's guide: Software for canonical community*  
760 *ordination (version 4.5)*. Microcomputer Power, Ithaca, New York.

761 Turkington, A.V. and Paradise, T.R. (2005) Sandstone weathering: A century of  
762 research and innovation. *Geomorphology*, 67, 229-253. Available at:  
763 doi:10.1016/j.geomorph.2004.09.028.

764 Vashista, M. and Paul, S. (2012) Correlation between full width at half  
765 maximum (FWHM) of XRD peak with residual stress on ground surfaces. *Philos.*  
766 *Mag.*, 92, 4194-4204. Available at: doi:10.1080/14786435.2012.704429.

767 Viles, H., Goudie, A., Grab, S. and Lalley, J. (2011) The use of the Schmidt  
768 Hammer and Equotip for rock hardness assessment in geomorphology and  
769 heritage science: A comparative analysis. *Earth Surf. Process. Landforms*, 36,  
770 320-333. Available at: doi:10.1002/esp.2040.

771 Viles, H. (2012) Microbial geomorphology: A neglected link between life and  
772 landscape. *Geomorphology*, 157, 6-16. Available at:  
773 doi:10.1016/j.geomorph.2011.03.021.

774 Viles, H. (2020) Biogeomorphology: Past, present and future. *Geomorphology*,  
775 366, 106809. Available at: doi:10.1016/j.geomorph.2019.06.022.

776 Wang, Y., Pei, Q., Yang, S., Guo, Q. and Viles, H. (2020) Evaluating the  
777 condition of sandstone Rock hewn cave temple facade using *in situ* non  
778 invasive techniques. *Rock Mech. Rock Eng.*, 53, 2915-2920. Available at:  
779 doi:10.1007/s00603-020-02063-w.

780 Weber, B., Scherr, C., Bicker, F., Friedl, T. and Buedel, B. (2011) Respiration-  
781 induced weathering patterns of two endolithically growing lichens. *Geobiology*,  
782 9, 34-43. Available at: doi:10.1111/j.1472-4669.2010.00256.x.

783 Whitlach, R.B. and Johnson, R.G. (1974) Methods for staining organic matter in  
784 marine sediments. *J. Sediment. Res.*, 44, 1310-1312. Available at:  
785 doi:10.1306/212F6CAD-2B24-11D7-8648000102C1865D.

786 Wierzchoś, J., de los Rios, A. and Ascaso, C. (2012) Microorganisms in desert  
787 rocks: The edge of life on Earth. *Int. Microbiol.*, 15, 171-181. Available at:  
788 doi:10.2436/20.1501.01.170.

789 Wilhelm, K., Viles, H. and Burke, O. (2016a) Low impact surface hardness  
790 testing (Equotip) on porous surfaces - Advances in methodology with

791 implications for rock weathering and stone deterioration research. *Earth Surf.*  
792 *Process. Landforms*, 41, 1027-1038. Available at: doi:10.1002/esp.3882.  
793 Wilhelm, K., Viles, H., Burke, O. and Mayaud, J. (2016b) Surface hardness as a  
794 proxy for weathering behaviour of limestone heritage: A case study on dated  
795 headstones on the Isle of Portland, UK. *Environ. Earth Sci.*, 75, 1-16. Available  
796 at: doi:10.1007/s12665-016-5661-y.  
797 Yun, T.S., Jeong, Y.J., Kim, K.Y. and Min, K.B. (2013) Evaluation of rock  
798 anisotropy using 3D X-ray computed tomography. *Eng. Geol.*, 163, 11-19.  
799 Available at: doi:10.1016/j.enggeo.2013.05.017.

800

## 801 **FIGURE CAPTIONS**

802

803 Fig. 1. Cross-sectioned Cortemilia sandstone blocks with visible impacts and  
804 sampling marks. (A) Right-angled surface obtained by cutting a block to  
805 expose its core as a model of the unweathered surface. (B) Series of Equotip  
806 measurements beneath a lichen thallus, close to the surface (i. 0.2-0.3 cm  
807 from the surface), at higher depth (ii. 1.0 cm from the surface), and in the  
808 block core (iii). (C) Powder sampling for XRPD analysis beneath lichen thallus  
809 (iv. 0.1-0.5 cm from the surface) and from the block core (v). Scale bar: 1 cm.  
810

811 Fig. 2. Relative stone hardness variation (RSH<sub>%</sub>) beneath lichens (*V.*  
812 *nigrescens*, Vn; *V. muralis*, Vm; *P. incrustans*, Pi) and biofilm control (BC), at  
813 different distances from the surface (0.2-0.3 cm, on the left; 1.0 cm, on the  
814 right). Box-plots which do not share at least one letter are statistically different  
815 (Kruskal-Wallis with Mann-Whitney U post hoc test; P<0.05).

816

817 Fig. 3. Penetration depth of *V. nigrescens* and *V. muralis* fungal component  
818 within stone surface. A. Difference among *V. nigrescens* and *V. muralis*  
819 penetration depth. B. *V. nigrescens* penetration patterns, with evident massive  
820 penetration of mycobiont hyphae red-stained by PAS coloration (within the  
821 dashed line). C. *V. muralis* penetration patterns, with algal clusters (asterisks)  
822 and perithecia (arrows) partially immersed in stone. Scale bars: 500 μm.

823

824 Fig. 4. XRPD analyses. A. Correlation of R<sub>Cc/Qz</sub> with stone hardness measured  
825 with Equotip for each sample. B. Ordination of samples on the basis of the  
826 percentage variation of I/FWHM ratio of each calcite peak referred to a  
827 crystallographic plane (PCoA vectors) with respect to the relative core sample.  
828 Median hardness (Leeb units) is annotated for each sample.

829

830 **TABLES**

831

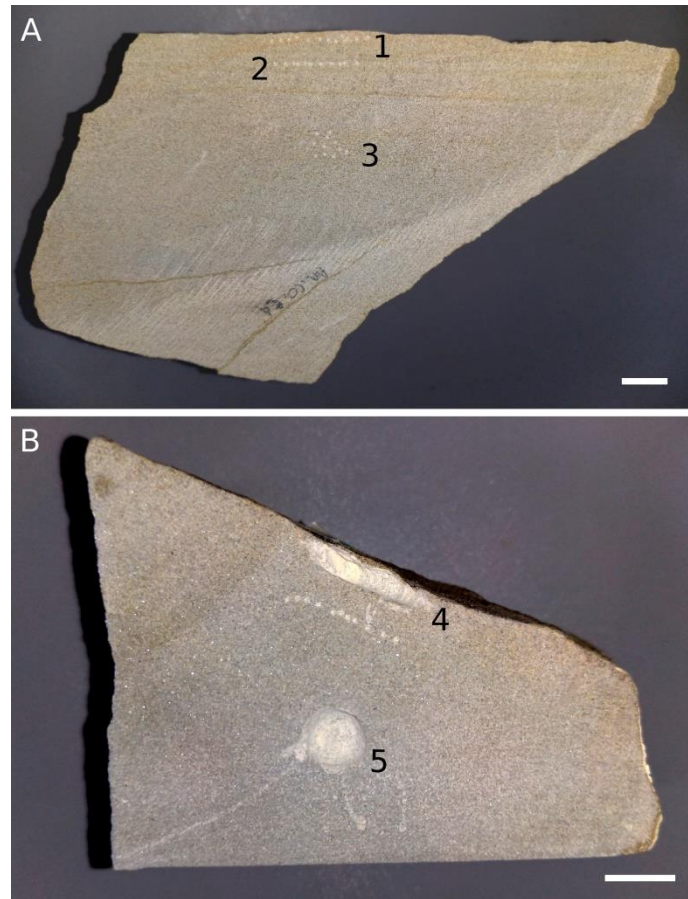
832 Table 1. Stone hardness variation measured on three Cortemilia sandstone  
 833 blocks under fresh, unweathered surfaces, to validate the method of impacting  
 834 close to the edge (0.2-0.3 cm) of the stone with Equotip Piccolo 2 (DL probe).  
 835 RSH<sub>%</sub> values represent hardness variation measured as ratio between median  
 836 edge hardness and core hardness, and is always negative and inferior to 1.2%.  
 837 Average  $\pm$ SD and RSD<sub>%</sub> are shown as informative measures of variance.

838

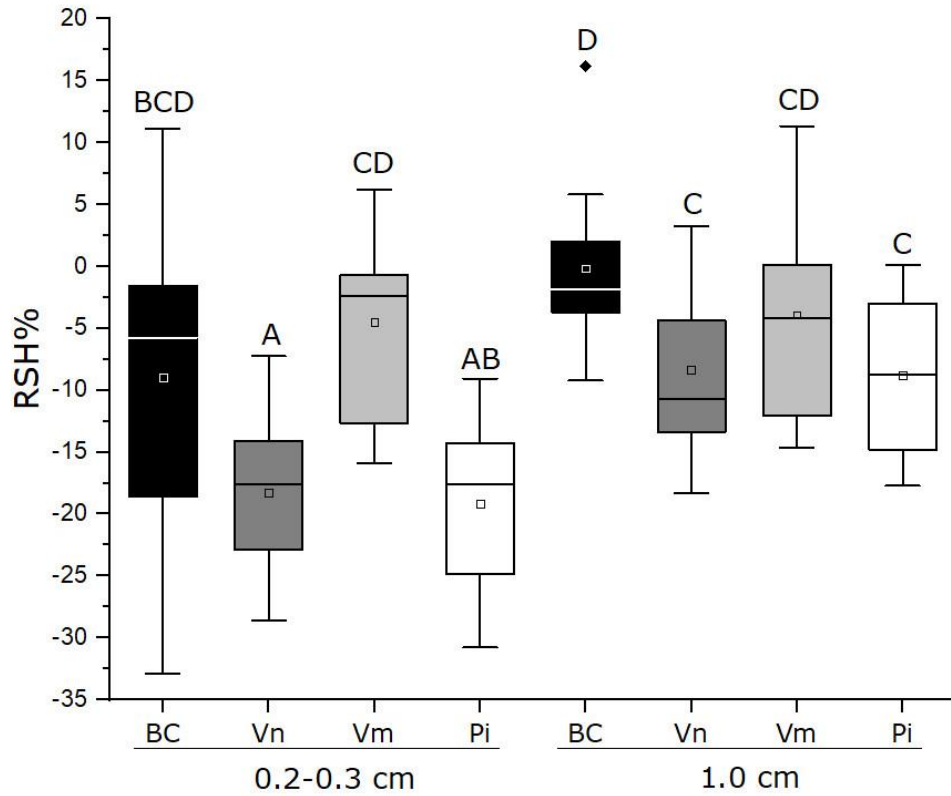
	Block F	Block J	Block Z
Core median (Leeb units)	722	683	764
Fresh edge median (Leeb units)	717	681	755
RSH <sub>%</sub>	-0.69%	-0.29%	-1.18%
Core average (Leeb units)	725.6	676.0	764.1
Core st.dev.	13.10	20.59	9.46
Core RSD <sub>%</sub>	1.8%	3.0%	1.2%
Fresh edge average (Leeb units)	723.1	683.5	752.8
Fresh edge st.dev.	13.60	24.25	10.66
Fresh edge RSD <sub>%</sub>	1.9%	3.5%	1.4%

839

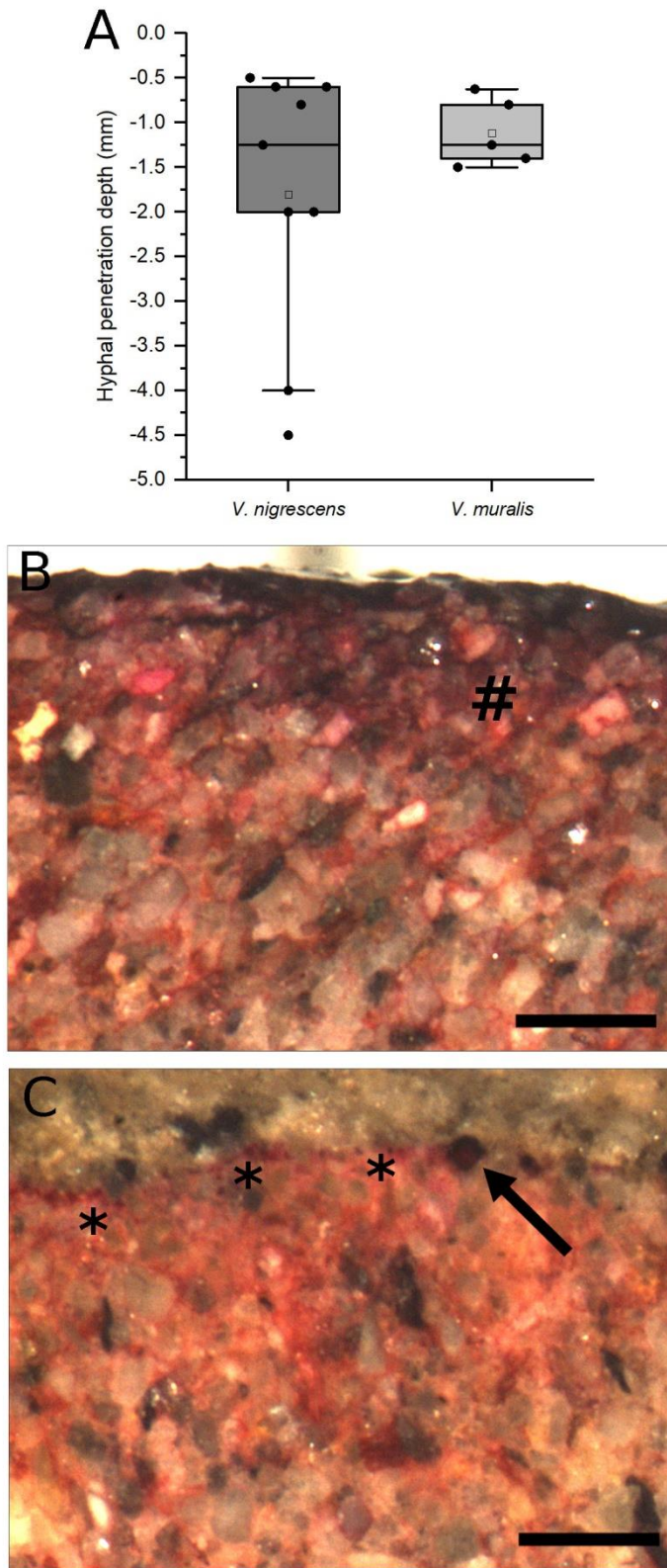
840



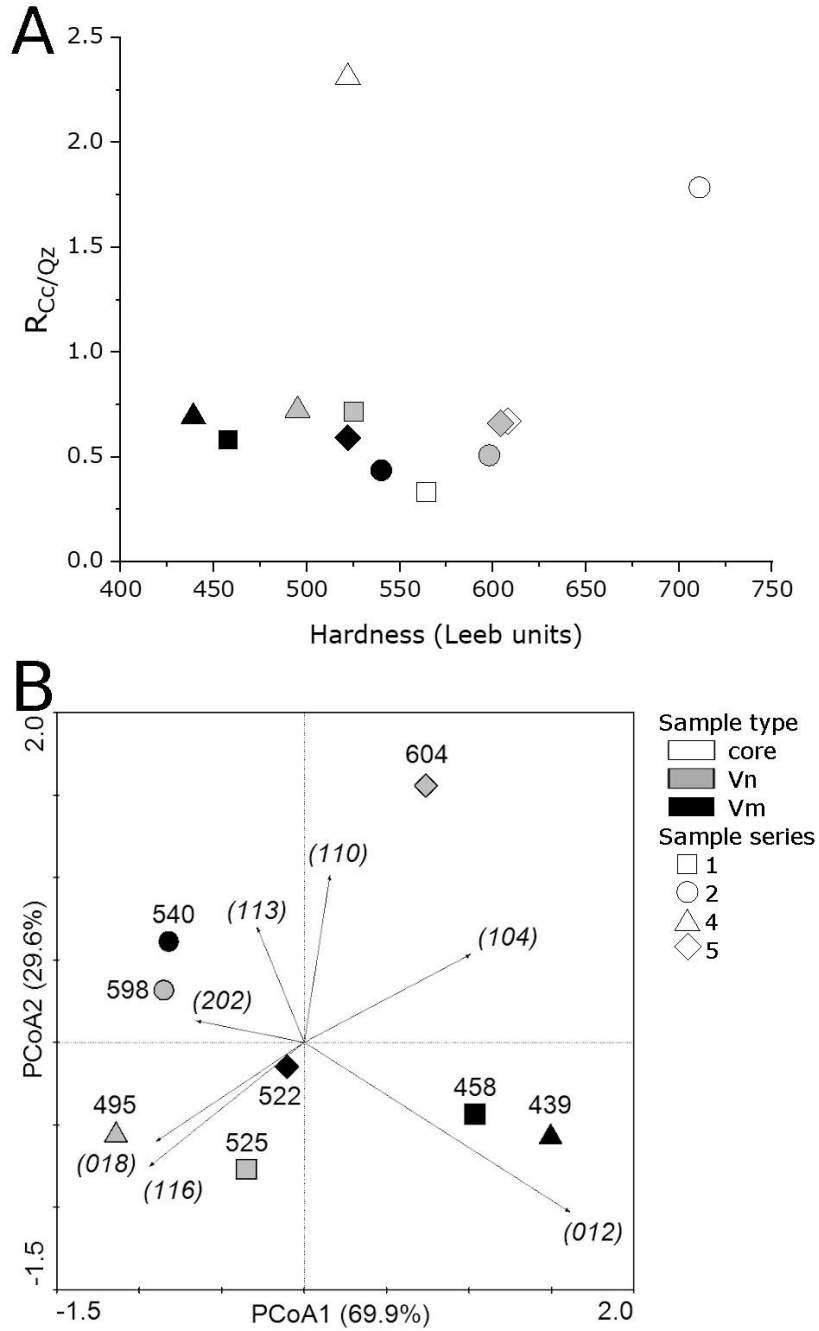
842  
 843 Fig. 1. Cross-sectioned Cortemilia sandstone blocks with visible impacts and sampling marks.  
 844 (A) Right-angled surface obtained by cutting a block to expose its core as a model of the  
 845 unweathered surface. (B) Series of Equotip measurements beneath a lichen thallus, close to  
 846 the surface ((i) 0.2–0.3 cm from the surface), at higher depth ((ii) 1.0 cm from the surface),  
 847 and in the block core (iii). (C) Powder sampling for XRPD analysis beneath lichen thallus ((iv)  
 848 0.1–0.5 cm from the surface) and from the block core (v). Scale bar: 1 cm  
 849



851 Fig. 2. Relative stone hardness variation (RSH%) beneath lichens (*V. nigrescens*, Vn; *V.*  
 852 *muralis*, Vm; *P. incrustans*, Pi) and biofilm control (BC), at different distances from the surface  
 853 (0.2-0.3 cm, on the left; 1.0 cm, on the right). Box-plots marked with different letters are  
 854 statistically different (Kruskal-Wallis with Mann-Whitney U post hoc test;  $P < 0.05$ ).  
 855



857 Fig. 3. Penetration depth of *V. nigrescens* and *V. muralis* fungal component within stone  
 858 surface. A. Difference among *V. nigrescens* and *V. muralis* penetration depth. B. *V. nigrescens*  
 859 penetration patterns, with evident massive penetration of mycobiont hyphae red-stained by  
 860 PAS coloration (within the dashed line). C. *V. muralis* penetration patterns, with algal clusters  
 861 (asterisks) and perithecia (arrows) partially immersed in stone. Scale bars: 500  $\mu$ m.  
 862



864  
 865 Fig. 4. XRPD analyses. A. Correlation of  $R_{Cc/Qz}$  with stone hardness measured with Equotip for  
 866 each sample. B. Ordination of samples on the basis of the percentage variation of I/FWHM  
 867 ratio of each calcite peak referred to a crystallographic plane (PCoA vectors) with respect to  
 868 the relative core sample. Median hardness (Leeb-units) is annotated for each sample.  
 869